Neurobiology of Disease

Dissociation of Metabolic and Neurovascular Responses to Levodopa in the Treatment of Parkinson's Disease

Shigeki Hirano,[1] Kotaro Asanuma,[1,2] Yilong Ma,[1,3] Chengke Tang,[1] Andrew Feigin,[1,3] Vijay Dhawan,[1,3] Maren Carbon,[1,3] and David Eidelberg[1,3]

[1]The Feinstein Institute for Medical Research, Manhasset, New York 11030, [2]Department of Neurology, Tokushima University Hospital, Tokushima 770-8503, Japan, and [3]Departments of Neurology and Medicine, North Shore University Hospital and New York University School of Medicine, New York, New York 10016

We compared the metabolic and neurovascular effects of levodopa (LD) therapy for Parkinson's disease (PD). Eleven PD patients were scanned with both [^{15}O]-H_2O and [^{18}F]-fluorodeoxyglucose positron emission tomography in the unmedicated state and during intravenous LD infusion. Images were used to quantify LD-mediated changes in the expression of motor- and cognition-related PD covariance patterns in scans of cerebral blood flow (CBF) and cerebral metabolic rate for glucose (CMR). These changes in network activity were compared with those occurring during subthalamic nucleus (STN) deep brain stimulation (DBS), and those observed in a test–retest PD control group. Separate voxel-based searches were conducted to identify individual regions with dissociated treatment-mediated changes in local cerebral blood flow and metabolism. We found a significant dissociation between CBF and CMR in the modulation of the PD motor-related network by LD treatment ($p < 0.001$). This dissociation was characterized by reductions in network activity in the CMR scans ($p < 0.003$) occurring concurrently with increases in the CBF scans ($p < 0.01$). Flow–metabolism dissociation was also evident at the regional level, with LD-mediated reductions in CMR and increases in CBF in the putamen/globus pallidus, dorsal midbrain/pons, STN, and ventral thalamus. CBF responses to LD in the putamen and pons were relatively greater in patients exhibiting drug-induced dyskinesia. In contrast, flow–metabolism dissociation was not present in the STN DBS treatment group or in the PD control group. These findings suggest that flow–metabolism dissociation is a distinctive feature of LD treatment. This phenomenon may be especially pronounced in patients with LD-induced dyskinesia.

Key words: **Parkinson's disease; positron emission tomography; glucose metabolism; cerebral blood flow; levodopa treatment; STN DBS**

Introduction

Functional imaging has increasingly been used as a means of objectively studying the effects of therapy for brain disease. In the resting condition, close correlations have been shown between steady-state measurements of regional cerebral metabolism and blood flow (Sokoloff, 1981; Raichle, 1998). Both measures are considered to be coupled to local synaptic activity (Jueptner and Weiller, 1995; Eidelberg et al., 1997; Sokoloff, 1999; Lin et al., 2008), supporting their use as treatment biomarkers (Herscovitch, 2001; Eckert and Eidelberg, 2005). Nonetheless, treatment can directly affect the cerebral vasculature as well as modulate neuronal activity. This consideration is particularly relevant for the use of imaging to the study of dopaminergic drugs for the treatment of Parkinson's disease (PD).

Experimental studies in rodent models have revealed localized increases in cerebral blood flow (CBF) with dopamine agonist drugs, as well as with dopamine itself (Ingvar et al., 1983; Tuor et al., 1986; Beck et al., 1988). Indeed, similar changes have been observed in both PD patients and normal subjects receiving levodopa (LD) (Leenders et al., 1985; Kobari et al., 1995; Hershey et al., 2003). These responses have been attributed to the direct effects of dopamine on the microvasculature, as supported by the demonstration of dopamine terminals apposed to arterioles and capillaries (Iadecola, 1998) (cf. Jones, 1982; Krimer et al., 1998) and of dopamine receptors on vessel walls (cf. Edvinsson and Krause, 2002).

These findings contrast with changes in regional metabolism observed with dopaminergic therapy. In the untreated state, PD is associated with increased cerebral metabolic rate for glucose (CMR) in the putamen, globus pallidus (GP), and ventral thalamus, as well as in the dorsal pons (Fukuda et al., 2001; Huang et al., 2007b) (cf. Porrino et al., 1990). These regional changes are thought to reflect localized increases in synaptic activity occurring within an abnormal metabolic brain network associated with the disease (cf. Eidelberg et al., 1994, 1997). Indeed, elevated expression of this PD-related spatial covariance pattern (PDRP) is reduced by dopaminergic therapy and by stereotaxic interventions targeting the hyperactive nodes of the network (Asanuma et al., 2006; Trošt et al., 2006; Feigin et al., 2007). The presence of

Received Jan. 7, 2008; revised Feb. 27, 2008; accepted Feb. 28, 2008.

This work was supported by National Institutes of Health–National Institute of Neurological Disorders and Stroke Grant R01 35069 (D.E.) and by the General Clinical Research Center of The Feinstein Institute for Medical Research (M01 RR018535). S.H. was supported by the Parkinson's Disease Foundation. Special thanks to Dr. Thomas Chaly for radiochemistry support and Ms. Toni Flanagan for manuscript preparation.

Correspondence should be addressed to David Eidelberg, The Feinstein Institute for Medical Research, 350 Community Drive, Manhasset, NY 11030. E-mail: david1@nshs.edu.

DOI:10.1523/JNEUROSCI.0582-08.2008

 0270-6474/08/284201-09$15.00/0

significant treatment-mediated metabolic reductions in these brain regions contrasts with the increases in CBF described above, and raises the possibility of dissociation in the two measures in response to therapy.

In this study, we measured CBF and CMR treatment responses in a group of PD patients undergoing a controlled LD infusion. Changes in these measures, as well as in quantitative indices of flow–metabolism dissociation during treatment, were compared with analogous changes in control patients studied twice on a stable medication dose. To determine whether these responses were specific for dopaminergic therapy, we compared the LD-mediated responses to those from a separate group of patients in whom a similar degree of clinical improvement was achieved with deep brain stimulation (DBS). Last, we explored the relationship of flow–metabolism dissociation to LD-induced dyskinesia (LID) by assessing the phenomenon in patients with and without this complication of therapy.

Table 1. Subject characteristics of the Parkinson's disease patients

Treatment groups	*n*	M:F	Age (years)	UPDRS[a] OFF	UPDRS[a] ON	Change (%)
Levodopa	11	8:3	60.4 (10.1)[b]	25.3 (8.0)	15.7 (6.0)	−38.2
Dyskinesia (−)	8	6:2	57.6 (8.9)	25.3 (9.3)	15.6 (6.8)	−37.4
Dyskinesia (+)	3	2:1	67.7 (11.0)	25.3 (4.6)	16.0 (2.8)	−41.0
STN DBS	8	7:1	64.7 (7.1)	31.6 (11.8)	21.0 (10.2)	−35.2
Test–retest	8	4:4	65.1 (9.1)		29.6 (13.8)[c]	

[a]Composite UPDRS motor ratings in a baseline state obtained 12 h after the cessation of antiparkinsonian medications (OFF) and in the treated state (ON).

[b]Mean ± SD.

[c]Test–retest assessments in the ON state (see Materials and Methods).

Materials and Methods

Subjects. We studied 11 PD patients before and during intravenous LD infusion. These patients underwent 2 consecutive days of positron emission tomography (PET) imaging in which scanning with both [^{15}O]-H_2O and [^{18}F]-fluorodeoxyglucose (FDG) was performed to respectively assess CBF and CMR in each treatment condition. On one day, imaging was conducted 12 h after the cessation of oral antiparkinsonian medications (OFF). On the other day, scanning was performed during an intravenous LD infusion (ON) titrated to achieve maximal improvement in Unified Parkinson's Disease Rating Scale (UPDRS) motor ratings (Feigin et al., 2001; Asanuma et al., 2006). The order of the ON and OFF PET sessions was randomized. On the ON days, the subjects received 200 mg of carbidopa orally 3 h before the start of the infusion, and an additional 50 mg 30 min beforehand. The mean infusion rate was 0.56 ± 0.04 mg/kg/h (mean ± SE). In eight of the patients there was no evidence of dyskinesia during either PET session; the three remaining patients exhibited sustained LID during the infusion. The infusion rate did not differ for patients with and without LID (0.57 ± 0.14 and 0.56 ± 0.04 mg/kg/h, respectively).

The PET data from the LD group were compared with those from two other PD cohorts. To compare LD to an intervention of similar efficacy, we studied 8 PD patients with bilateral STN DBS electrodes. These patients underwent PET imaging with both tracers in separate baseline (OFF) and bilateral stimulation (ON) sessions, each conducted 12 h after the last medication dose. The effect of STN stimulation on motor signs was similar to that achieved with LD (mean change in motor UPDRS ratings of 10.6 points, −35.2%, and 10.0 points, −38.2%, respectively, for the two interventions; $p < 0.001$), without dyskinesias. Details of these experiments, including the stimulation parameters used in the ON-state studies, have been published previously (Asanuma et al., 2006).

The PET data from the active interventions (LD and STN DBS) were compared with data from a group of eight PD control subjects with stable responses to oral dopaminergic therapy without dyskinesia. These subjects underwent repeat PET imaging in two sessions separated by 8 weeks (Ma et al., 2007). In each session, PET imaging with both tracers was conducted in the ON state, after routine morning medication. Medication doses were not altered between sessions.

Demographic and clinical features of the patients in the three treatment groups (LD, STN DBS, PD control) are presented in Table 1. In these subjects, the diagnosis of PD was made according to standard criteria (Hughes et al., 1992); they all exhibited ≥20% improvement in UPDRS motor ratings with dopaminergic therapy. Limited metabolic data from these patients have appeared previously (Feigin et al., 2001; Asanuma et al., 2006; Ma et al., 2007).

Positron emission tomography. Subjects fasted overnight before each PET session. For the LD and STN DBS groups, antiparkinsonian medications were withheld at least 12 h before PET. For the PD control group, patients were scanned on the same dose of oral medication in the two PET sessions. Imaging was performed in three-dimensional mode using a GE Advance tomograph (GE Medical Systems, Milwaukee, WI). This eight-ring bismuth germanate scanner provided 35 two-dimensional image planes with axial field view of 14.5 cm and transaxial resolution of 4.2 mm in all directions. All PET studies were performed in the rest state with the subjects' eyes open in a dimly lit room with minimal auditory stimulation.

To estimate CBF, we used a modification of the slow bolus method in which 10 mCi of [^{15}O]-H_2O was injected as described previously (Carbon et al., 2007). CBF scans were repeated twice in each treatment condition. The interval between the two [^{15}O]-H_2O administrations was at least 10 min to allow for the decay of radioactivity. In each session, the [^{15}O]-H_2O scans were followed by an [^{18}F]-FDG PET study for the measurement of CMR. In each FDG PET study, scan acquisition began 35 min after the injection of 5 mCi radiotracer and continued for 10 min. Ethical permission for the studies was obtained from the Institutional Review Board of North Shore University Hospital. Written consent was obtained from each subject after detailed explanation of the procedures.

Data analysis. Imaging data processing was performed using SPM99 (Wellcome Department of Cognitive Neurology, London, UK) implemented in Matlab 6.1 (MathWorks, Sherborn, MA). The scans from each subject were realigned separately and nonlinearly warped into Talairach space (Talairach and Tournoux, 1988) and were smoothed with an isotropic Gaussian kernel for all directions [full width at half maximum (FWHM) 10 mm for [^{18}F]-FDG; FWHM 15 mm for [^{15}O]-H_2O] to improve the signal-to-noise ratio.

Network analysis. For each PD patient group and treatment condition, we quantified the expression of spatial covariance patterns associated with the motor and cognitive manifestations of the disease (Eckert et al., 2007). These metabolic networks, known as the PD motor- and cognition-related spatial covariance patterns (PDRP and PDCP, respectively) (Fig. 1), have been validated in previous PET studies (Huang et al., 2007a,b) (cf. Feigin et al., 2007). Network activity was assessed in all scans using a fully automated voxel-based algorithm (software available at http://www.feinsteinneuroscience.org/software) (Ma et al., 2007). These network computations were performed blinded to treatment group (LD, STN DBS, PD control), condition (OFF and ON for LD and STN DBS patients; test and retest for PD controls), scan (CBF and CMR), and clinical status (UPDRS motor ratings). We also computed network scores in nine healthy volunteer subjects (4 men and 5 women; age: 56.0 ± 13.8 years) who underwent PET imaging with both [^{15}O]-H_2O and [^{18}F]-FDG in a single session. For both CBF and CMR scans, individual values for the PD patients were offset by subtracting the average value of the healthy subjects so that the control mean was zero for each network. For each group, treatment-mediated changes in network activity measured in the CBF and CMR scans were compared by using a two-way 2 × 2 (condition × scan) repeated-measures ANOVA (RMANOVA) with *post hoc* Bonferroni tests. In each model, treatment condition (ON/OFF; test/retest) was defined as the within-subject repeated measure and scan (CBF and CMR) defined as the between-subjects variable.

Treatment-mediated changes in PDRP and PDCP expression were

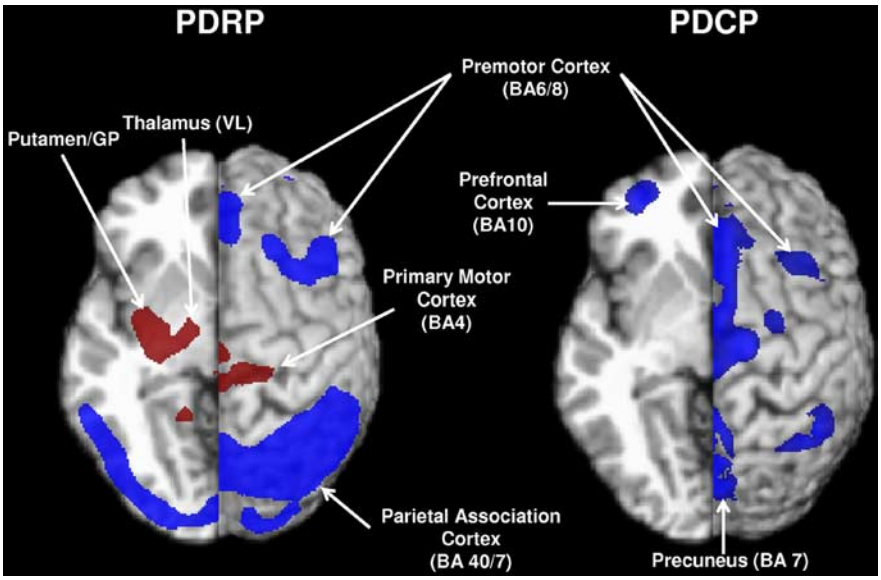

Figure 1. Left, PDRP (Ma et al., 2007) was characterized by pallidothalamic, pontine, and motor cortical hypermetabolism, associated with relative metabolic reductions in the lateral premotor and posterior parietal areas. Right, PDCP (Huang et al., 2007a) was characterized by hypometabolism of prefrontal cortex, rostral supplementary motor area, and superior parietal regions. Relative metabolic increases are displayed in red; relative metabolic decreases are displayed in blue. Both patterns were overlaid on a standard magnetic resonance imaging brain template. The left hemisphere was cut in the transverse plane at z = −5 mm. The right hemisphere was displayed as a surface projection on the same brain template. BA, Brodmann's area.

computed separately in the CBF and CMR scans (Δ_{CBF} and Δ_{CMR}) of each patient by subtracting scores for the ON and OFF sessions (ON − OFF for the LD and STN DBS groups), or for the repeat scan sessions (scan 2 − scan 1 for the PD control group). The network changes within each group were also separately correlated with disease duration and UPDRS motor ratings by computing Pearson product moment correlation coefficients. For each subject, we also quantified a network-based descriptor of flow–metabolism dissociation during treatment. This dissociation index (DI) was defined as $\Delta_{CBF} - \Delta_{CMR}$ and was determined separately for the PDRP and PDCP networks. For both patterns, a DI value of 0 indicated equal treatment-mediated changes in network activity for the CBF and the CMR scan data. Positive DI values indicated greater treatment-mediated changes in blood flow relative to metabolism ($\Delta_{CBF} > \Delta_{CMR}$), whereas negative values indicated the opposite ($\Delta_{CBF} < \Delta_{CMR}$). Differences in DI across treatment groups were assessed using a one-way ANOVA followed by *post hoc* Bonferroni tests.

In addition, differences in network activity between groups (i.e., LD vs STN DBS; LD vs PD control) were evaluated by directly comparing PDRP/PDCP expression in the LD group with analogous values measured in the STN DBS or the PD control groups. This was done using separate three-way 2 × 2 × 2 (condition × group × scan) RMANOVA models in which treatment condition (ON/OFF; test/retest) was defined as the within-subject repeated measure, and treatment group (LD, STN DBS, PD control) and scan (CBF, CMR) were defined as the between-subjects variables. If, for each three-way RMANOVA, a significant three-way interaction effect was found, two subsequent 2 × 2 (condition × group) RMANOVAs were separately performed for the CBF and CMR scans incorporating *post hoc* Bonferroni tests.

Regional analysis. To localize brain regions in which there was significant dissociation between CBF and CMR during treatment, we performed an interaction analysis of the [^{15}O]-H_2O and [^{18}F]-FDG PET data from each group (LD, STN DBS, PD control). Scans from both treatment conditions (OFF/ON or test/retest) were globally normalized at a threshold of 0.8 and interrogated for the following interaction effects: $[(CBF_{ON} - CBF_{OFF}) > (CMR_{ON} - CMR_{OFF})]$ and $[(CBF_{ON} - CBF_{OFF}) < (CMR_{ON} - CMR_{OFF})]$, represented by the contrasts [1,−1,−1,1] and [−1,1,1,−1], respectively. Areas with significant interaction effects were reported at a threshold of $p < 0.05$, corrected for multiple comparisons. We also reported regional interaction effects at an uncorrected threshold of $p < 0.001$ with minimum cluster size of 50 voxels. This hypothesis-testing threshold was used to evaluate submaxima located within anatomical regions in which significant treatment-mediated changes in CBF and/or CMR had been reported previously (Hershey et al., 1998, 2003; Huang et al., 2007b).

Significant brain regions were further analyzed with *post hoc* volume of interest (VOI) assessments. Functional activity (CBF or CMR) was measured within a sphere (radius, 3 mm) centered on the peak voxel for each significant region. The resulting local VOI values were normalized by the global value for each scan and examined for the presence of interaction effects using a two-way 2 × 2 (condition × scan) RMANOVA followed by *post hoc* Bonferroni tests. For all regions, normalized VOI values were also compared with corresponding values from the healthy control cohort using an analysis of covariance (ANCOVA) model with estimates of global CBF and CMR as covariates to adjust for possible group differences in these measures. Left and right regional control values were averaged for these comparisons, which were considered significant for $p < 0.05$.

Effects of levodopa-induced dyskinesia. In the regions with significant interaction effects, we computed regional DI values (i.e., $\Delta_{CBF} - \Delta_{CMR}$) for treatment-mediated changes in globally normalized VOI values. We compared these values from the three LID patients to analogous values from their LD-treated counterparts without dyskinesia (DYS−) and from the control subjects. To avoid making incorrect inferences regarding the LID patients based on their DYS- counterparts, we only analyzed VOIs in which the regional DI for DYS− differed from PD controls at a significance level of $p < 0.01$ (two-way 2 × 2 RMANOVA). In these regions, we inspected the individual subject Δ_{CBF} and Δ_{CMR} data to determine whether values for the LID patients differed qualitatively from those of the other patients (DYS− and PD controls). We also examined the normalized CBF and CMR values from these regions in both treatment conditions (ON and OFF) to determine the relationship of the LID values to those from the DYS− and the healthy control groups. In addition, ON- and OFF-state values for the LID patients were separately compared with values for the PD and the healthy control groups using a one-way ANCOVA with global CBF/CMR as a covariate. Values for the three LID patients were displayed graphically with reference to the means for the DYS− and for the PD control subjects.

All statistical analyses were performed in SPSS 9.0 (SPSS, Chicago, IL) and the results were considered significant at $p < 0.05$.

Results

Flow–metabolism dissociation: network effects

Treatment-mediated changes in PDRP expression in the patient groups (LD, STN DBS, and PD control) are presented in Figure 2*A*. LD-mediated changes in PDRP expression differed significantly in the CMR and CBF scan data ($F_{(1,20)} = 20.8$, $p < 0.001$; two-way RMANOVA) (Fig. 2*A*, left). Flow–metabolism dissociation with LD treatment was characterized by reductions in network activity in the CMR scans ($p < 0.003$; *post hoc* Bonferroni test) associated with concurrent increases in the CBF scans ($p \leq 0.01$). This dissociation remained significant ($p < 0.001$) when the analysis was restricted to the nondyskinetic (DYS−) patients. In the LD-treatment group, network-related changes in the CBF scans correlated with disease duration ($r = 0.75$, $p = 0.01$) (Fig. 2*B*), but not with changes in motor ratings ($r = -0.32$, $p = 0.35$).

Network-related changes in the CMR data did not correlate with these measures ($|r| < 0.43$, $p > 0.22$).

Despite giving rise to clinical improvement comparable with LD, bilateral STN stimulation (Fig. 2*A*, middle) did not result in dissociation of treatment-mediated PDRP responses in the CMR and CBF scan data (interaction effect: $F_{(1,14)} = 0.02$, $p = 0.90$; two-way RMANOVA). Indeed, with STN stimulation (Fig. 2*A*, middle), PDRP expression declined relative to baseline in both the CMR and CBF scans ($p < 0.04$; *post hoc* Bonferroni test for each scan type). As expected, there was no change in PDRP activity in the test–retest PD control data, whether in repeat CBF or CMR scans ($p > 0.33$) (Fig. 2*A*, right).

For the PDRP, the DI (i.e., $\Delta_{CBF} - \Delta_{CMR}$ for treatment-mediated changes in network activity) differed significantly across the three groups ($F_{(2,24)} = 7.47$, $p < 0.004$; one-way ANOVA). This measure (Fig. 2*C*) was greater in the LD group relative to the STN DBS ($p < 0.04$) and the PD control groups ($p < 0.005$). These group differences were substantiated in the subsequent RMANOVAs, which revealed significant three-way (condition × scan × group) interaction effects for the comparison of LD to STN DBS ($F_{(1,34)} = 5.89$, $p < 0.03$) and the comparison of LD to the PD controls ($F_{(1,34)} = 13.3$, $p < 0.001$). Additional analysis revealed that the LD-mediated increases in PDRP activity observed in the CBF scans differed significantly from the reductions seen in the same scan data with STN stimulation ($F_{(1,17)} = 5.85$, $p < 0.03$; two-way RMANOVA) and from the test–retest variability of the PD controls ($F_{(1,17)} = 5.06$, $p < 0.04$). In contrast, in the CMR scans, LD was associated with a reduction in PDRP expression, which was not different from that observed with STN stimulation ($F_{(1,17)} = 0.66$, $p = 0.43$). These LD-mediated changes did however differ from those measured in the PD control group ($F_{(1,17)} = 9.62$, $p < 0.007$).

In contrast to the PDRP, there were no significant treatment-mediated changes in PDCP activity in scans from any of the groups ($p > 0.36$). Moreover, for this network, DI values (Fig. 2*D*) did not differ across the three treatment groups ($F_{(2,24)} = 0.04$, $p = 0.96$; one-way ANOVA).

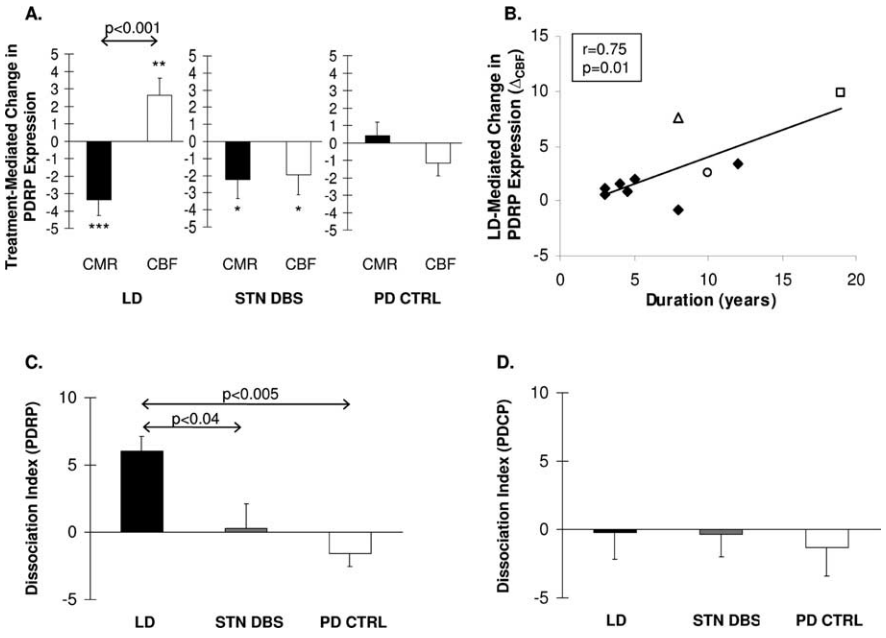

Figure 2. ***A***, Bar graph illustrating mean treatment-mediated changes in the expression of the PDRP measured in scans of CMR (filled bars) and CBF (open bars). At the network level, a significant dissociation between the CMR and CBF treatment responses ($p < 0.001$) is present with LD (left), but not with STN DBS (middle) or in PD controls (PD CTRL) (right) undergoing repeat imaging on stable doses of dopaminergic medication. ***$p < 0.005$; **$p < 0.01$; *$p < 0.05$, *post hoc* Bonferonni comparisons of ON versus OFF values for each treatment group. ***B***, Correlation between disease duration and PDRP-related CBF increases during levodopa (LD) infusion (Δ_{CBF}; see text). A significant correlation ($r = 0.75$, $p = 0.01$) was found between these variables. PD patients undergoing LD infusion with or without dyskinesia are represented by open and filled symbols, respectively. ***C***, Bar graph illustrating measures of flow–metabolism dissociation during treatment for the motor-related PDRP network (see Materials and Methods). The dissociation index was significantly different for the three groups ($p < 0.004$), with greater dissociation in the LD group (filled bar) relative to both STN stimulation (gray bar) ($p < 0.04$) and PD controls (open bar) ($p < 0.005$). ***D***, None of the three groups exhibited significant flow–metabolism dissociation in the response of the PDCP. Error bars indicate SEM.

Flow–metabolism dissociation: global and regional effects

Estimated global values for CMR and CBF did not change with either LD infusion ($F_{(1,20)} = 0.001$, $p = 0.97$) or STN stimulation ($F_{(1,20)} = 0.32$, $p = 0.58$). These values also did not change on repeat testing in the PD control group ($F_{(1,20)} = 1.48$, $p = 0.25$). Likewise, global DI values (i.e., $\Delta_{CBF} - \Delta_{CMR}$ for treatment-mediated changes in the global values) did not differ across the three groups ($F_{(2,24)} = 0.35$, $p = 0.71$; one-way ANOVA). Voxel-based searches were conducted in each group to identify brain regions in which treatment gave rise to dissociated changes in CMR and CBF. Significant regional interaction effects were detected in the LD group (Table 2), but not in the STN DBS or the PD control groups. With LD, all significant regional interaction effects involved reductions in glucose metabolism occurring concurrently with increases in blood flow. Dissociation of treatment responses in the opposite direction was not encountered.

LD-mediated dissociation of CBF and CMR ($p < 0.001$, cluster-level corrected) was detected in the left posterolateral putamen, extending medially into the adjacent GP and ventral thalamus (Fig. 3*A*, top). A homologous region was identified in the right posterior putamen. LD infusion was also associated with significant flow–metabolism dissociation in the dorsal pons ($p < 0.005$, cluster-level corrected), involving the locus ceruleus and elements of the pedunculopontine nucleus (Fig. 3*A*, bottom). This cluster extended rostrally to include the dorsal raphe and the subthalamic region. Significant interaction effects ($p < 0.001$, uncorrected) remained in all the reported regions when the analysis was limited to DYS− patients.

The presence of significant dissociation of LD-mediated CMR and CBF treatment responses in these areas was confirmed on subsequent VOI analysis ($F_{(1,20)} > 15.0$, $p \leq 0.001$; two-way RMANOVA). In each VOI, the regional dissociation effect remained significant after excluding the three LID patients ($F_{(1,14)} > 11.0$, $p < 0.005$). In the putamen/GP, the LD-mediated decrease in CMR was similar in magnitude to the increase in CBF (−5.8% and +6.3%, respectively) (Fig. 3*B*, top left). Although of relatively smaller magnitude (absolute value ≤4.0%), treatment responses in the ventral thalamus and STN were also similar for CMR and CBF (Fig. 3*B*, right). In contrast, in the dorsal pons, LD infusion was associated with greater effects on CBF (+8.6%) relative to CMR (−2.8%) (Fig. 3*B*, bottom left).

In all of these areas, normalized OFF-state CMR values for the

Table 2. Brain regions with significant flow–metabolism dissociation during levodopa treatment

	Coordinates[a]			Zmax	CMR[b]		CBF[c]	
	x	*y*	*z*		LD (OFF)	LD (ON)	LD (OFF)	LD (ON)
Putamen/GP	−30	−8	2	4.82****	2.01 (0.05)	1.89 (0.05)†††	1.70 (0.02)	1.80 (0.04)†††
	32	−4	−2	3.63**	2.05 (0.05)	1.95 (0.05)†	1.78 (0.03)	1.85 (0.04)†
Thalamus	12	−22	0	3.05*	1.88 (0.04)	1.80 (0.03)†	1.81 (0.03)	1.86 (0.03)†
Subthalamic nucleus	10	−10	−4	2.88*	1.49 (0.04)	1.44 (0.03)††	1.62 (0.03)	1.67 (0.03)†
Dorsal pons	6	−34	−32	4.85***	1.36 (0.04)	1.32 (0.03)†	1.61 (0.03)	1.74 (0.04)†††

[a]Montreal Neurological Institute (MNI) standard space.

[b]Globally normalized CMR for glucose (mean ± SE) in each VOI (see Materials and Methods).

[c]Globally normalized CBF (mean ± SE) in each VOI (see Materials and Methods).

Significant flow–metabolism dissociation (SPM interaction analysis): *$p < 0.001$, uncorrected; **$p < 0.05$, extent corrected; ***$p < 0.005$, ****$p < 0.001$, cluster corrected with voxel-level familywise error correction ($p < 0.05$).
Significant ON–OFF differences (paired *t* test): $^{\dagger}p < 0.05$; $^{\dagger\dagger}p < 0.01$; $^{\dagger\dagger\dagger}p < 0.001$.

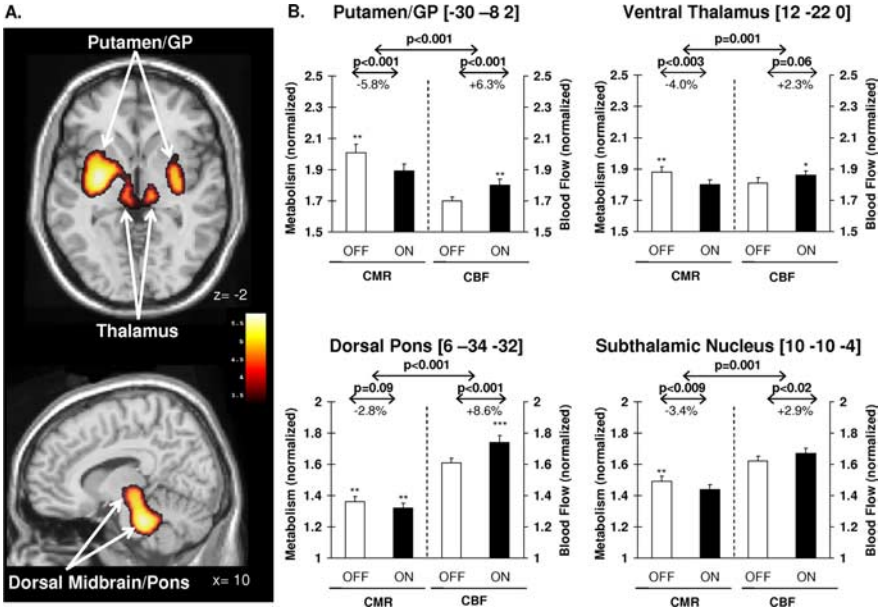

Figure 3. ***A***, Results of voxel-based searches for brain regions with significant flow–metabolism dissociation in response to levodopa therapy. Top, Treatment-mediated dissociation of regional glucose metabolism and cerebral blood flow is present bilaterally in the posterior-lateral putamen and adjacent GP, and in the ventral thalamus. Bottom, Significant dissociation effects with levodopa are also present in the dorsal pons and midbrain. Metabolic increases are displayed using a red–yellow scale. Both displays were superimposed on a single-subject magnetic resonance imaging brain template and thresholded at $t = 3.28$, $p = 0.001$, extent threshold >50 voxels (peak voxel, uncorrected). ***B***, Bar graphs of globally normalized cerebral glucose metabolism (CMR) and blood flow (CBF) in VOIs centered on the peak voxel for each of these regions (see Materials and Methods). In all VOIs, significant LD-mediated reductions in regional metabolism were associated with concurrent increases in blood flow. Baseline values (±SE) measured 12 h after medication withdrawal (OFF) are represented by open bars. Values on an optimized LD infusion (ON) are represented by filled bars. ***$p < 0.001$; **$p < 0.01$; *$p < 0.05$ for comparisons with healthy control values. Error bars indicate SEM.

LD patients were elevated relative to the healthy controls ($F_{(1,17)} > 8.36$, $p \leq 0.01$; ANCOVA adjusted for group differences in global CMR). In the putamen/GP, dorsal pons, and thalamus, normalized ON-state CBF values were also elevated relative to healthy controls ($F_{(1,17)} > 6.30$, $p < 0.001$ for the pons, $p < 0.01$ for the putamen/GP, and $p < 0.05$ for the thalamus; ANCOVA adjusted for group differences in global CBF). In these patients, global CBF and CMR for both treatment conditions (ON and OFF) did not differ from healthy control values ($p > 0.22$).

Flow–metabolism dissociation: relationship to levodopa-induced dyskinesia

We first assessed flow–metabolism dissociation in the absence of LID by comparing regional DI values in DYS− patients with PD controls. We found that significant treatment-mediated dissociation was present in the putamen/GP and dorsal pons of the DYS− patients relative to the test–retest controls ($p < 0.001$ and $p < 0.01$ for the two regions, respectively; two-way RMANOVA). Notably, in these regions, the three LID patients (open symbols) displayed greater flow–metabolism dissociation than their DYS− counterparts (Fig. 4*A*). Indeed, the LID patients had the highest DI values of the entire LD treatment group. Further inspection of the data revealed that in both regions, the three LID patients also had relatively larger CBF treatment responses (Δ_{CBF}) than their DYS− counterparts (Fig. 4*B*). In contrast, CMR treatment responses (Δ_{CMR}) in the LID patients were similar to those for the DYS− patients. This suggests that the greater degree of dissociation seen with LID was driven by the relatively larger CBF treatment responses observed in these patients.

Based on these findings, we examined the normalized CBF data from these regions in both the ON and OFF treatment conditions. We found that in the ON state, normalized CBF values for the DYS−, PD control, and normal control groups (Fig. 4*C*) differed significantly in the pons ($F_{(2,21)} = 12.9$, $p < 0.001$; ANCOVA adjusted for group differences in global CBF), but only marginally in the putamen/GP ($F_{(2,21)} = 3.27$, $p = 0.06$). In the pons, DYS− values were elevated relative to healthy controls ($p < 0.001$); whereas in the putamen/GP, these elevations did not reach significance ($p = 0.06$; *post hoc* Bonferroni test). In both regions, ON-state values for the DYS− patients were similar to those for the PD controls ($p = 0.99$), who were also studied while on medication.

We note that in both regions, individual ON-state normalized CBF values for the LID patients (open symbols) were higher than for the DYS− and the PD control groups, with elevations >2.4 SD above the healthy control mean. Indeed, including the three LID patients in these comparisons improved the results of ANCOVA for both regions (pons: $F_{2,24} = 16.09$, $p < 0.001$; putamen/GP: $F_{(2,24)} = 9.06$, $p = 0.001$). This is particularly true for the putamen/GP, where the entire LD group (LID plus DYS− patients) exhibited significant CBF elevations relative to the healthy controls ($p < 0.02$; *post hoc* Bonferroni test), compared with the marginal elevations seen in the DYS− patients alone (see above).

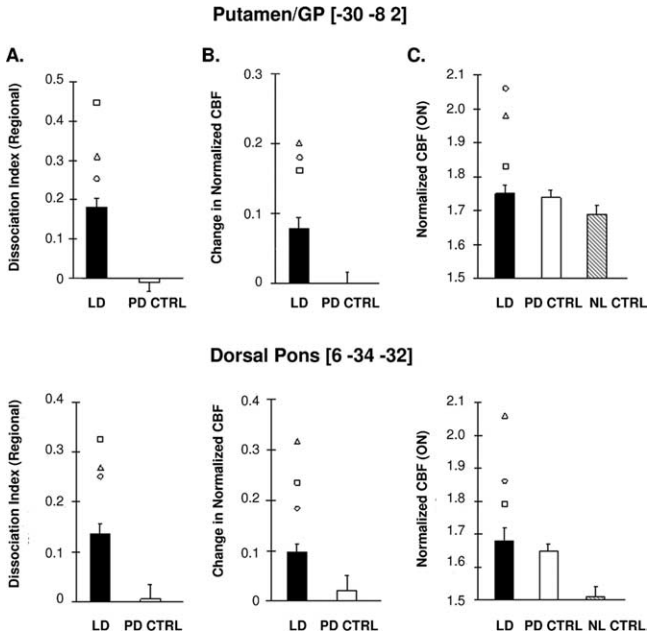

Figure 4. Displays of regional brain data from patients with and without dyskinesia scanned during levodopa infusion. ***A***, Flow–metabolism dissociation. In the putamen/GP (top) and dorsal pons (bottom), patients without dyskinesia (DYS−; filled bars) exhibited significant flow–metabolism dissociation during treatment compared with PD controls (PD CTRL; open bars) undergoing repeat testing on medication. In both regions, the LID patients (open symbols) consistently displayed greater flow–metabolism dissociation than their DYS-counterparts. ***B***, Vasomotor response. In these regions, the DYS− patients exhibited treatment-mediated increases in normalized CBF relative to the PD controls. Relative to DYS−, the LID patients had consistently larger CBF responses to treatment while not displaying a consistent difference in their CMR responses. ***C***, Normalized CBF. In the putamen/GP (top), ON-state values were marginally elevated ($p = 0.06$) in the DYS− patients relative to normal controls (NL CTRL; shaded bars). However, these values were considerably higher in the LID patients, leading to the significant elevation ($p < 0.02$) that was observed for the whole LD group. In contrast, in the pons (bottom), these values were already abnormally elevated ($p < 0.001$) even without the LID patients. In both regions, normalized CBF values were similar for the DYS- and the PD control (PD CTRL; open bars) patients. Error bars indicate SEM.

In contrast, in both regions, OFF-state normalized CBF values did not differ for the LD patients (with or without including LID) relative to controls (pons: $p > 0.20$; putamen/GP: $p > 0.53$; ANCOVA).

Discussion

Metabolic and vasomotor responses to levodopa therapy

In this study, we describe a significant dissociation of the metabolic and neurovascular effects of dopaminergic therapy for PD. Our data also indicate that this effect is highly specific at both the network and regional levels. Regarding the former, flow–metabolism dissociation with LD treatment was restricted to the PDRP, a spatial covariance pattern linked to the motor effects of antiparkinsonian therapy (Carbon et al., 2003; Asanuma et al., 2006; Feigin et al., 2007). In contrast, the activity of the cognition-related PD network (PDCP) did not exhibit treatment-mediated dissociation in any of the patient groups.

The treatment-mediated dissociation effects within the PDRP were highly region specific. In our whole brain voxel-by-voxel search, only a few brain areas exhibited significant dissociation of CBF and CMR in response to LD. These regions, the putamen and adjacent pallidum, the dorsal pons and midbrain, and the STN and ventral thalamus, were found to share a number of distinct features. First, baseline metabolic activity in these regions was elevated in PD patients relative to healthy controls (Fig. 3, asterisks) (cf. Fukuda et al., 2001; Huang et al., 2007b), consistent with increases in local afferent synaptic activity (Eidelberg et al., 1997) (cf. Jueptner and Weiller, 1995; Sokoloff, 1999). Metabolic increases in these regions can be viewed as reflecting disease-related overactivity of corticostriatal, STN-pallidal, and pallidothalamic and pontine projection pathways within the PDRP network (Huang et al., 2007b; Lin et al., 2008). Second, nerve terminals in these regions are known to express L-aromatic amino acid decarboxylase (AADC) to varying degrees (Jaeger et al., 1984; Smith and Kieval, 2000) (cf. Brown et al., 1999; Rakshi et al., 1999; Garcia-Cabezas et al., 2007).

Our data suggest that a spatial correspondence exists between the brain regions with significant flow–metabolism dissociation during LD treatment and those with elevations in synaptic activity and retained local AADC expression. This point is illustrated in Figure 5, in which abnormal OFF-state elevations in regional glucose utilization (green) were mapped alongside areas (red) with high specific [^{18}F]-fluorodopa (FDOPA) uptake, a PET index of AADC activity (Dhawan et al., 1996; Ishikawa et al., 1996). Areas of overlap between these measures (yellow, top) (i.e., regions with both functional characteristics) corresponded closely to those exhibiting significant LD-mediated dissociation in the current sample (blue, bottom). This suggests that flow–metabolism dissociation occurs in regions with baseline elevations in synaptic activity (as is the case in the hypermetabolic nodes of the PDRP) in which there is also sufficient enzymatic capacity to decarboxylate LD to dopamine. In these areas, significant treatment-mediated metabolic reductions are accompanied by dissociated increases in CBF linked to local dopamine production. Interestingly, dissociated treatment responses were not present at all PDRP nodes. For instance, baseline elevations in glucose metabolism are present in the sensorimotor cortex (Asanuma et al., 2006; Huang et al., 2007b), whereas FDOPA signal is not especially pronounced in this region. In contrast, FDOPA uptake is high in the anterior cingulate cortex (Rakshi et al., 1999), but baseline metabolic activity is not elevated there. In both cases, significant flow–metabolism dissociation was not evident in our data.

We propose that the local increases in CBF that occur as part of the LD treatment response are mediated through direct contacts between monaminergic terminals and the microvasculature. Specifically, AADC is expressed within dopaminergic and serotonergic striatal terminals, wherein exogenous LD can be converted to dopamine, either directly or as a "false neurotransmitter" (Carta et al., 2007). Given the close proximity of these terminals to adjacent capillaries (Jones, 1982; Krimer et al., 1998), the released dopamine can act directly on vascular receptors. Alternatively, dopamine released into the intersynaptic cleft may, in the setting of low DAT binding, spill over and diffuse over large distances to act on more distant microvessels (Cragg and Rice, 2004) (cf. Schneider et al., 1994). High concentrations of dopamine generally result in vasoconstriction. Nonetheless, lower concentrations, such as those associated with systemic LD infusion, are more likely to have a vasodilatory action (von Essen et al., 1980; Toda, 1983; cf. Edvinsson and Krause, 2002). Similar effects can be considered in other regions in which monoaminergic terminals and/or dendrites appose nearby blood vessels, such as the locus ceruleus, midbrain raphe, and substantia nigra (Felten and Crutcher, 1979; Jones, 1982), as well as the ventral thalamic nuclei (Garcia-Cabezas et al., 2007).

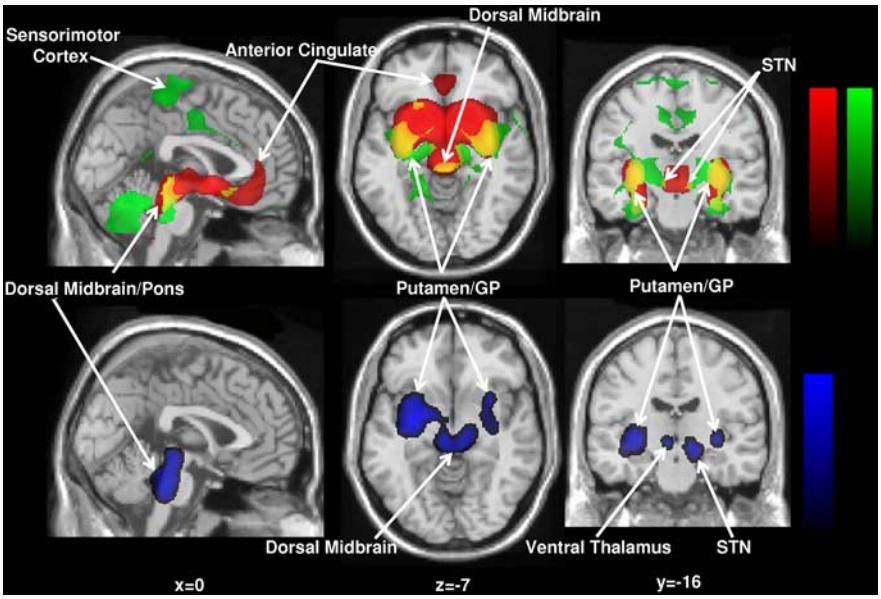

Figure 5. Top, Display of brain areas (green) with significant elevations in regional glucose metabolism relative to healthy control subjects. These clusters were identified in a voxel-based comparison of FDG PET scans from 20 unmedicated PD patients with those from 20 age-matched healthy subjects (Fukuda et al., 2001). Brain areas with retained AADC activity (red) were identified in a separate voxel-based analysis of FDOPA PET data from 11 PD patients (age, 55.1 ± 9.6; OFF-state motor UPDRS, 27.9 ± 11.3) matched to the current LD treatment group. These scans were used to map regions with elevated radiotracer uptake relative to background. Areas of overlap between the two statistical maps (yellow) indicate regions in which elevated synaptic activity and local AADC expression are both present. Bottom, Display of brain areas (blue) with significant levodopa-mediated flow–metabolism dissociation. These clusters were identified in the current LD treatment cohort using a voxel-based interaction analysis (see Materials and Methods). There is a spatial correspondence between these areas and the overlapping regions (yellow) displayed in the top panel. For each map, the voxel displays were thresholded at $z = 3.5$, $p < 0.001$ and superimposed on a standard magnetic resonance imaging template.

Flow–metabolism dissociation and complications of levodopa therapy

The relevance of flow–metabolism dissociation to PD treatment is not known. Although significant dissociation was evident in the putamen/GP and dorsal pons during uncomplicated LD therapy, this effect was more pronounced in the three LID patients. Indeed, inspection of the globally normalized CMR and CBF data showed that the heightened dissociation observed in these patients was associated with substantially increased treatment-mediated vasomotor responses (Δ_{CBF}) and concomitant elevations in ON-state regional CBF measures. Interestingly, in the putamen/GP, the LID patients showed higher ON-state CBF values than those observed in the nondyskinetic PD patients and the healthy controls. Including these patients in the analysis greatly enhanced the significance of the local CBF elevation that was observed in the LD group relative to the healthy controls. This suggests that LID is associated with the increased vasomotor effect of treatment seen in this region. In contrast, in the pons, PD patients without dyskinesia already showed significant CBF abnormalities which were not appreciably strengthened by including the LID patients in the comparison with healthy control subjects. Thus, although LID patients also had very high CBF values in this region, the effect was not specific for dyskinesia. This is consistent with similar pontine CBF elevations observed in healthy subjects treated with oral LD (Hershey et al., 2003). Additionally, the finding of significant ON-state elevations in thalamic CBF is compatible with the results of a previous study in which LD-mediated CBF responses in LID patients were compared with their nondyskinetic counterparts (Hershey et al., 1998).

The presence of significant LD-mediated dissociation in nondyskinetic patient argues against this phenomenon as a secondary effect of the dyskinesias themselves. Likewise, the correlation between disease duration and the magnitude of the vasomotor response to LD (Fig. 2*B*) suggests that flow–metabolism dissociation is an ongoing process that likely antecedes the development of LID. That said, there are several potential explanations for the development of LID in some subjects and not others. For one thing, individual differences in the density of monoaminergic innervation of the microvasculature could determine the potential for vasodilation during LD administration. This source of intersubject variability would be present from birth and have little to do with the manifestations of PD that occur later in life. Another possibility relates to differences in vascular density occurring as part of the disease process or as a by-product of dopamine therapy (Barcia et al., 2005) (cf. Faucheux et al., 1999). It has been suggested previously that LID is associated with endothelial proliferation triggered by the stimulation of dopamine receptors on blood vessels in LD-treated animals (Westin et al., 2006). In this vein, angiogenesis represents a response to the long-term alterations in synaptic activity that underlie this disease and its treatment (cf. Black et al., 1991). Nonetheless, we did not find a change in regional perfusion in the LID patients when they were scanned off medication. Indeed, the CBF abnormalities found in these patients were evident only in the ON state. Thus, one may need to consider the possibility that new vessels are particularly sensitive to the vasoactive effects of dopamine, or that they are associated with leakage of LD across the blood–brain barrier (Carvey et al., 2005; Wang et al., 2005). Additional studies in experimental animal models and PD patients will be needed to test these hypotheses and their relevance to the human disease.

We note that LID is associated with increased putaminal dopamine release after LD administration (de la Fuente-Fernandez et al., 2004), which might directly contribute to the regional increases in CBF that were observed. That said, excess delivery of LD to the putamen is not necessarily benign, as suggested by a recent experimental study of LID (Carta et al., 2006). Along these lines, one can speculate that blocking the vasomotor effects of LD treatment may improve treatment-mediated dyskinesia. It is interesting that several agents proposed for the treatment of LID have potent vasoconstrictive features that may be regionally selective. For instance, α_2 adrenoceptor antagonists have been proposed as a means of treating LID by blocking the effects of noradrenaline on striatal output neurons (Fox et al., 2001). These receptors are known to be widely present on blood vessels and can facilitate vasodilation (Zou and Cowley, 2000). Thus, antagonists like idazoxan may potentially block this effect and selectively reduce perfusion to areas rich in vascular α_2 adrenoceptors (Bryan et al., 1996). Similar considerations may also apply to nicotine, another drug with potent vasoconstrictive effects that has been observed to have antidyskinetic properties (Quik et al., 2007).

Additional research will be needed to clarify the role of vasomotor mechanisms in the pathogenesis and treatment of LID.

References

Asanuma K, Tang C, Ma Y, Dhawan V, Mattis P, Edwards C, Kaplitt MG, Feigin A, Eidelberg D (2006) Network modulation in the treatment of Parkinson's disease. Brain 129:2667–2678.

Barcia C, Bautista V, Sanchez-Bahillo A, Fernandez-Villalba E, Faucheux B, Poza y Poza M, Fernandez Barreiro A, Hirsch EC, Herrero MT (2005) Changes in vascularization in substantia nigra pars compacta of monkeys rendered parkinsonian. J Neural Transm 112:1237–1248.

Beck T, Vogg P, Krieglstein J (1988) Uncoupling of cerebral blood flow and glucose utilization by dihydroergocristine in the conscious rat. Naunyn Schmiedebergs Arch Pharmacol 338:82–87.

Black JE, Zelazny AM, Greenough WT (1991) Capillary and mitochondrial support of neural plasticity in adult rat visual cortex. Exp Neurol 111:204–209.

Brown WD, Taylor MD, Roberts AD, Oakes TR, Schueller MJ, Holden JE, Malischke LM, DeJesus OT, Nickles RJ (1999) FluoroDOPA PET shows the nondopaminergic as well as dopaminergic destinations of levodopa. Neurology 53:1212–1218.

Bryan Jr RM, Eichler MY, Swafford MW, Johnson TD, Suresh MS, Childres WF (1996) Stimulation of alpha 2 adrenoceptors dilates the rat middle cerebral artery. Anesthesiology 85:82–90.

Carbon M, Edwards C, Eidelberg D (2003) Functional brain imaging in Parkinson's disease. Adv Neurol 91:175–181.

Carbon M, Ghilardi MF, Dhawan V, Eidelberg D (2007) Correlates of movement initiation and velocity in Parkinson's disease: a longitudinal PET study. NeuroImage 34:361–370.

Carta M, Lindgren HS, Lundblad M, Stancampiano R, Fadda F, Cenci MA (2006) Role of striatal L-DOPA in the production of dyskinesia in 6-hydroxydopamine lesioned rats. J Neurochem 96:1718–1727.

Carta M, Carlsson T, Kirik D, Bjorklund A (2007) Dopamine released from 5-HT terminals is the cause of L-DOPA-induced dyskinesia in parkinsonian rats. Brain 130:1819–1833.

Carvey PM, Zhao CH, Hendey B, Lum H, Trachtenberg J, Desai BS, Snyder J, Zhu YG, Ling ZD (2005) 6-Hydroxydopamine-induced alterations in blood–brain barrier permeability. Eur J Neurosci 22:1158–1168.

Cragg SJ, Rice ME (2004) DAncing past the DAT at a DA synapse. Trends Neurosci 27:270–277.

de la Fuente-Fernandez R, Sossi V, Huang Z, Furtado S, Lu JQ, Calne DB, Ruth TJ, Stoessl AJ (2004) Levodopa-induced changes in synaptic dopamine levels increase with progression of Parkinson's disease: implications for dyskinesias. Brain 127:2747–2754.

Dhawan V, Ishikawa T, Patlak C, Chaly T, Robeson W, Belakhlef A, Margouleff C, Mandel F, Eidelberg D (1996) Combined FDOPA and 3OMFD PET studies in Parkinson's disease. J Nucl Med 37:209–216.

Eckert T, Eidelberg D (2005) Neuroimaging and therapeutics in movement disorders. NeuroRx 2:361–371.

Eckert T, Tang C, Eidelberg D (2007) Assessment of the progression of Parkinson's disease: a metabolic network approach. Lancet Neurol 6:926–932.

Edvinsson L, Krause D (2002) Catecholamines. In: Cerebral blood flow and metabolism (Edvinsson L, Krause D, eds), pp 191–211. Philadelphia, PA: Lippincott, Williams and Wilkins.

Eidelberg D, Moeller JR, Dhawan V, Spetsieris P, Takikawa S, Ishikawa T, Chaly T, Robeson W, Margouleff D, Przedborski S, Fahn S (1994) The metabolic topography of parkinsonism. J Cereb Blood Flow Metab 14:783–801.

Eidelberg D, Moeller JR, Kazumata K, Antonini A, Sterio D, Dhawan V, Spetsieris P, Alterman R, Kelly PJ, Dogali M, Fazzini E, Beric A (1997) Metabolic correlates of pallidal neuronal activity in Parkinson's disease. Brain 120:1315–1324.

Faucheux BA, Bonnet AM, Agid Y, Hirsch EC (1999) Blood vessels change in the mesencephalon of patients with Parkinson's disease. Lancet 353:981–982.

Feigin A, Fukuda M, Dhawan V, Przedborski S, Jackson-Lewis V, Mentis MJ, Moeller JR, Eidelberg D (2001) Metabolic correlates of levodopa response in Parkinson's disease. Neurology 57:2083–2088.

Feigin A, Kaplitt MG, Tang C, Lin T, Mattis P, Dhawan V, During MJ, Eidelberg D (2007) Modulation of metabolic brain networks after subthalamic gene therapy for Parkinson's disease. Proc Natl Acad Sci USA 104:19559–19564.

Felten DL, Crutcher KA (1979) Neuronal-vascular relationships in the raphe nuclei, locus coeruleus, and substantia nigra in primates. Am J Anat 155:467–481.

Fox SH, Henry B, Hill MP, Peggs D, Crossman AR, Brotchie JM (2001) Neural mechanisms underlying peak-dose dyskinesia induced by levodopa and apomorphine are distinct: evidence from the effects of the alpha(2) adrenoceptor antagonist idazoxan. Mov Disord 16:642–650.

Fukuda M, Mentis MJ, Ma Y, Dhawan V, Antonini A, Lang AE, Lozano AM, Hammerstad J, Lyons K, Koller WC, Moeller JR, Eidelberg D (2001) Networks mediating the clinical effects of pallidal brain stimulation for Parkinson's disease: a PET study of resting state glucose metabolism. Brain 124:1601–1609.

Garcia-Cabezas MA, Rico B, Sanchez-Gonzalez MA, Cavada C (2007) Distribution of the dopamine innervation in the macaque and human thalamus. NeuroImage 34:965–984.

Herscovitch P (2001) Can [15O]water be used to evaluate drugs? J Clin Pharmacol [Suppl] 41:11S–20S.

Hershey T, Black KJ, Stambuk MK, Carl JL, McGee-Minnich LA, Perlmutter JS (1998) Altered thalamic response to levodopa in Parkinson's patients with dopa-induced dyskinesias. Proc Natl Acad Sci USA 95:12016–12021.

Hershey T, Black KJ, Carl JL, McGee-Minnich L, Snyder AZ, Perlmutter JS (2003) Long term treatment and disease severity change brain responses to levodopa in Parkinson's disease. J Neurol Neurosurg Psychiatry 74:844–851.

Huang C, Mattis P, Tang C, Perrine K, Carbon M, Eidelberg D (2007a) Metabolic brain networks associated with cognitive function in Parkinson's disease. Neuroimage 34:714–723.

Huang C, Tang C, Feigin A, Lesser M, Ma Y, Pourfar M, Dhawan V, Eidelberg D (2007b) Changes in network activity with the progression of Parkinson's disease. Brain 130:1834–1846.

Hughes AJ, Daniel SE, Kilford L, Lees AJ (1992) Accuracy of clinical diagnosis of idiopathic Parkinson's disease: a clinico-pathological study of 100 cases. J Neurol Neurosurg Psychiatry 55:181–184.

Iadecola C (1998) Neurogenic control of the cerebral microcirculation: is dopamine minding the store? Nat Neurosci 1:263–265.

Ingvar M, Lindvall O, Stenevi U (1983) Apomorphine-induced changes in local cerebral blood flow in normal rats and after lesions of the dopaminergic nigrostriatal bundle. Brain Res 262:259–265.

Ishikawa T, Dhawan V, Chaly T, Margouleff C, Robeson W, Dahl JR, Mandel F, Spetsieris P, Eidelberg D (1996) Clinical significance of striatal DOPA decarboxylase activity in Parkinson's disease. J Nucl Med 37:216–222.

Jaeger CB, Ruggiero DA, Albert VR, Park DH, Joh TH, Reis DJ (1984) Aromatic L-amino acid decarboxylase in the rat brain: immunocytochemical localization in neurons of the brain stem. Neuroscience 11:691–713.

Jones BE (1982) Relationship between catecholamine neurons and cerebral blood vessels studied by their simultaneous fluorescent revelation in the rat brainstem. Brain Res Bulletin 9:33–44.

Jueptner M, Weiller C (1995) Rev: does measurement of regional cerebral blood flow reflect synaptic activity? Implications for PET and fMRI. NeuroImage 2:148–156.

Kobari M, Fukuuchi Y, Shinohara T, Obara K, Nogawa S (1995) Levodopa-induced local cerebral blood flow changes in Parkinson's disease and related disorders. J Neurol Sci 128:212–218.

Krimer LS, Muly III EC, Williams GV, Goldman-Rakic PS (1998) Dopaminergic regulation of cerebral cortical microcirculation. Nat Neurosci 1:286–289.

Leenders KL, Wolfson L, Gibbs JM, Wise RJ, Causon R, Jones T, Legg NJ (1985) The effects of L-DOPA on regional cerebral blood flow and oxygen metabolism in patients with Parkinson's disease. Brain 108:171–191.

Lin TP, Carbon M, Tang C, Mogilner AY, Sterio D, Beric A, Dhawan V, Eidelberg D (2008) Metabolic correlates of subthalamic nucleus activity in Parkinson's disease. Brain, in press.

Ma Y, Tang C, Spetsieris PG, Dhawan V, Eidelberg D (2007) Abnormal metabolic network activity in Parkinson's disease: test-retest reproducibility. J Cereb Blood Flow Metab 27:597–605.

Porrino LJ, Huston-Lyons D, Bain G, Sokoloff L, Kornetsky C (1990) The distribution of changes in local cerebral energy metabolism associated with brain stimulation reward to the medial forebrain bundle of the rat. Brain Res 511:1–6.

Quik M, Cox H, Parameswaran N, O'Leary K, Langston JW, Di Monte D

(2007) Nicotine reduces levodopa-induced dyskinesias in lesioned monkeys. Ann Neurol 62:588–596.

Raichle ME (1998) Behind the scenes of functional brain imaging: a historical and physiological perspective. Proc Natl Acad Sci USA 95:765–772.

Rakshi JS, Uema T, Ito K, Bailey DL, Morrish PK, Ashburner J, Dagher A, Jenkins IH, Friston KJ, Brooks DJ (1999) Frontal, midbrain and striatal dopaminergic function in early and advanced Parkinson's disease A 3D [(18)F]dopa-PET study. Brain 122:1637–1650.

Schneider JS, Rothblat DS, DiStefano L (1994) Volume transmission of dopamine over large distances may contribute to recovery from experimental parkinsonism. Brain Res 643:86–91.

Smith Y, Kieval JZ (2000) Anatomy of the dopamine system in the basal ganglia. Trends Neurosci 23:S28–33.

Sokoloff L (1981) Localization of functional activity in the central nervous system by measurement of glucose utilization with radioactive deoxyglucose. J Cereb Blood Flow Metab 1:7–36.

Sokoloff L (1999) Energetics of functional activation in neural tissues. Neurochem Res 24:321–329.

Talairach J, Tournoux P (1988) Coplanar stereotaxic atlas of the human brain. Stuttgart, Germany: Thieme.

Toda N (1983) Heterogeneity in the response to dopamine of monkey cerebral and peripheral arteries. Am J Physiol 245:H930–H936.

Trošt M, Su S, Su P, Yen RF, Tseng HM, Barnes A, Ma Y, Eidelberg D (2006) Network modulation by the subthalamic nucleus in the treatment of Parkinson's disease. NeuroImage 31:301–307.

Tuor UI, Edvinsson L, McCulloch J (1986) Catecholamines and the relationship between cerebral blood flow and glucose use. Am J Physiol 251:H824–H833.

von Essen C, Zervas NT, Brown DR, Koltun WA, Pickren KS (1980) Local cerebral blood flow in the dog during intravenous infusion of dopamine. Surg Neurol 13:181–188.

Wang Y, Kilic E, Kilic U, Weber B, Bassetti CL, Marti HH, Hermann DM (2005) VEGF overexpression induces post-ischaemic neuroprotection, but facilitates haemodynamic steal phenomena. Brain 128:52–63.

Westin JE, Lindgren HS, Gardi J, Nyengaard JR, Brundin P, Mohapel P, Cenci MA (2006) Endothelial proliferation and increased blood-brain barrier permeability in the basal ganglia in a rat model of 3,4-dihydroxyphenyl-L-alanine-induced dyskinesia. J Neurosci 26:9448–9461.

Zou AP, Cowley Jr AW (2000) α(2)-adrenergic receptor-mediated increase in NO production buffers renal medullary vasoconstriction. Am J Physiol Regul Integr Comp Physiol 279:R769–R777.